BIOTECHNOLOGY PROCESSES

Scale-up and Mixing

Edited by
CHESTER S. HO
JAMES Y. OLDSHUE

BIOTECHNOLOGY PROCESSES

Scale-up and Mixing

Edited by

CHESTER S. HO
State University of New York at Buffalo
Buffalo, N.Y.

JAMES Y. OLDSHUE
Mixing Equipment Company
Rochester, New York

American Institute of Chemical Engineers
New York, New York

Library of Congress Cataloging-in-Publication Data

Biotechnology processes.

Includes index.

1. Biochemical engineering—Congresses. 2. Biotechnology—Methodology—Congresses. I. Ho, Chester S., 1950– . II. Oldshue, James Y. III. American Institute of Chemical Engineers.

TP248.3.B62 1987 660'.6 87-14393

ISBN 0–8169–0410–3

MANUFACTURED IN THE UNITED STATES OF AMERICA

BIOTECHNOLOGY PROCESSES

Scale-up and Mixing

Preface

The American Institute of Chemical Engineers held a major symposium on Scale-up and Mixing of Bioprocesses at the Miami annual meeting in November, 1986. The sessions attracted twenty presentations. Another seven, which were not included in the oral presentations, are included in the volume. This represents a major collection of twenty-seven papers that relate to many different aspects of chemical engineering in bioprocessing.

The papers encompass experimental and design work on existing fermentors, which include the typical aerobic process well known in the industry. Results of studies of the mixing characteristics include a variety of experimental observations with different kinds of impellers, particularly the high pumping capacity, low shear rate impellers introduced in the last three or four years. These are usually patterned after airfoil designs, and are typically called either hydrofoil, liquidfoil, or laserfoil impeller.

Scale-up is a key item in bioprocessing, and several papers discuss the principles of scale-up and give examples of various types of scale-up calculations.

Some of the latest bioprocesses involve mammalian cells or other biological organisms that are much more sensitive to fluid shear stress than previously well-known free-suspending organisms. This may well indicate a different kind of impeller system, particularly where aerobic requirements are either low or absent, and the mixer is to provide primarily a blending and cell suspension function. The characteristics of airlift, airpulse, and bubble columns are included in the contributions presented in this volume. Of additional interest are methods of handling the non-Newtonian character of many fluids in bioprocessing. A variety of papers in this volume look at some of the basic concepts of mass transfer in impeller mixed fermentors as well as airlift types.

Particularly encouraging is a large number of papers devoted to actual bioprocess operations. These include descriptions of the requirements for several different products. Also very encouraging is the large number of papers from industrial sources, and the data presented which will be of help to all concerned in the pursuit of information in the whole spectrum of bioprocessing.

The editors would like to thank the authors for their fine contributions, and their diligent attention to time schedules and proper form for the paper preparation which made the production of this book a reality. The helpful suggestions and assistance of the AIChE staff and Stanley Barnett of the University of Rhode Island are also acknowledged.

Chester S. Ho
State University of New York at Buffalo
Buffalo, N.Y.

James Y. Oldshue
Mixing Equipment Company
Rochester, N.Y.

Contents

BIOPROCESS SCALE-UP

BIOPROCESS APPLICATIONS

BIOPROCESS MIXING

Stirred Bioreactors

Current Situation in Fluid Mixing for Fermentation Processes

JAMES Y. OLDSHUE
Mixing Equipment Company
Rochester, New York

Fermentation involves anaerobic and aerobic processes. In anaerobic processes there is no need for high oxygen uptake rates and the main mixer design parameters are involved with mass transfer across the liquid-solid boundary, possible effects of shear rate on the organisms, and the overall blending and mixing of nutrients in the tank.

The main consideration with looking at mixer designs is to examine the role of fluid shear, power and pumping capacity.

Looking first at turbulent flow situations, in which the Reynolds number around the impeller is 1,000 or higher, we can take a measurement of the velocity at a point and we will normally get a fluctuating velocity as shown in Figure 1. From this fluctuating velocity profile with time, we can calculate the average velocity as well as the fluctuating component. The fluctuating component is normally expressed as a root mean square velocity fluctuation.

It turns out that large particles (on the order of 1,000 microns or larger) see only the average velocity and the velocity gradients between adjacent layers of fluid. These are shown in Figure 2 and it is seen that around a radial flow impeller, that there is a maximum shear rate, related to tip speed, and an average shear rate related to impeller operating speed.

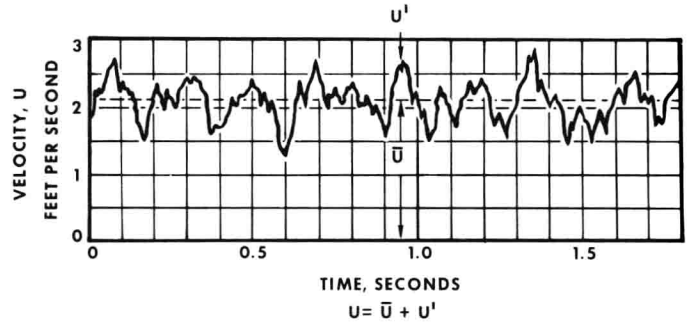

FIGURE 1. Typical velocity fluctuation in turbulent flow.

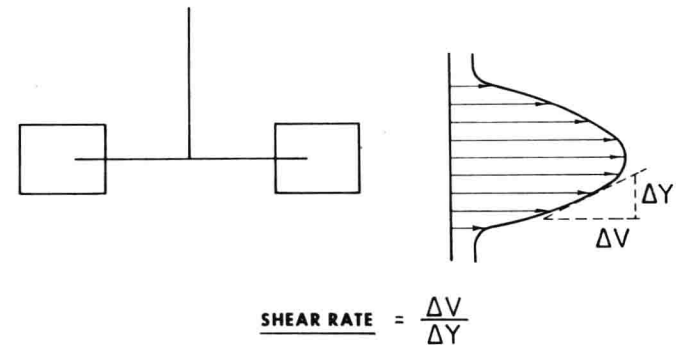

FIGURE 2. Method of calculation of average and maximum macro scale impeller zone shear rates.

All the power dissipates as heat. The only way to go from heat to power is through viscous shear. Therefore, the velocity gradients that affect the large scale particles, the macro scale, do not absorb a large part of the energy. The energy, which is represented by power per unit of volume, is largely dissipated through the action of the turbulent small scale viscous shear rates, which are related to the root mean square velocity fluctuation.

Micro scale shear rates affect particles largely 100 microns or smaller and are related in a major way to the power per unit of volume, as well as the root mean square velocity fluctuations.

The large particles respond to the macro scale shear rates based on average velocities, and don't know in general that the micro scale shear rates exist. On the other hand, small scale particles go along for the ride on the macro scale velocities, but respond directly to the high frequency fluctuations that are in their size regime.

The old saying that you must match the shear stresses and the responses to the particles is involved here; that you don't use a rivet hammer drill tooth--you don't use an ultrasonic drill to drive a rivet.

Every mixing problem has a micro scale mixing floor which is necessary to carry out the proper combination of fluid particles and materials at micro scale levels. It can also be very responsive to the micro scale level, and so process results can markedly change by power per unit of volume. On the other hand, many of the other combinations of functions are related to shear rates on a macro scale basis.

In the pilot plant the purpose is usually to determine which variables are the most important. This means that the scale of the pilot plant is very important. For macro scale mixing processes, the impeller blades should physically be at least three times bigger than the biggest particle, bubble, droplet or fluid clump that is of interest to the process. Otherwise, scaling will not be relative to what will happen in the full scale system.

A small mixing tank has a very short blend time and a much lower maximum shear rate impeller zone relative to large tanks. It may be necessary to use a non-geometric impeller and mixing tank on a small scale to duplicate the performance of proper variables on full scale.

Sufficient oxygen mass transfer is usually no problem in aerobic systems in the pilot plant. Without regard to scale, comparable mass transfer rates per unit of volume can be achieved on small and large systems. The main problem comes into the blending phenomena. The large tank has a much longer blend time than the small tank and this can lead to oxygen deficiencies in remote parts of the tank. Mass transfer zones should be made a part of the overall mixing flow pattern in the entire system.

In terms of minimum fluid shear rates required for some mammalian cells, and other types of shear sensitive cells, there will need to be a different approach to mixing requirements.

There is a whole family of fluid foil impellers, Figure 3, which are able to produce motion with the very least amount of shear rate--both macro and micro scale. However, if these impellers are required on small scale, then the same questions that existed previously, "how do we keep the blend time at a high enough and reasonable level on full scale and the shear rates down to a reasonable maximum on full scale?" apply to these impellers as well.

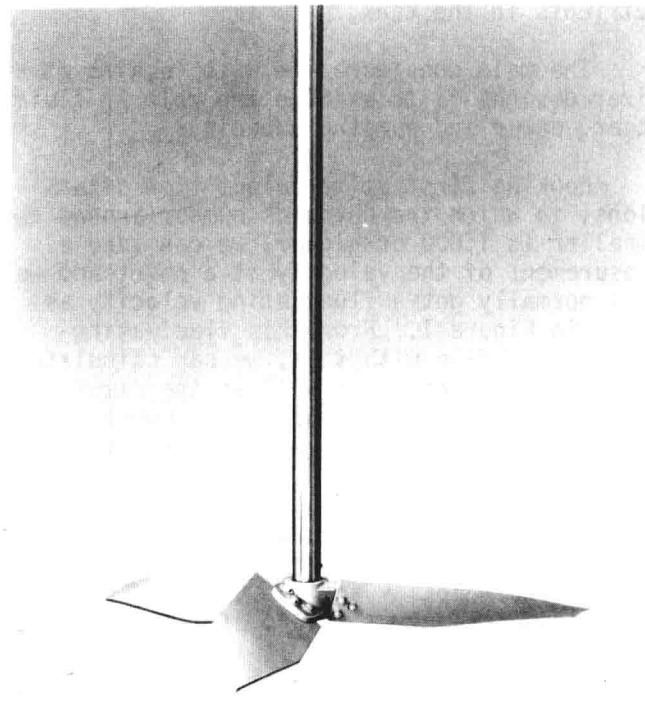

FIGURE 3. Typical fluid foil impeller.

There are other kinds of impellers such as anchors, Figure 4, and helicals. Figure 5, that have a much different kind of shear rate and flow pattern. These impellers may well end up to be the impellers of choice in cultures that are very shear sensitive.

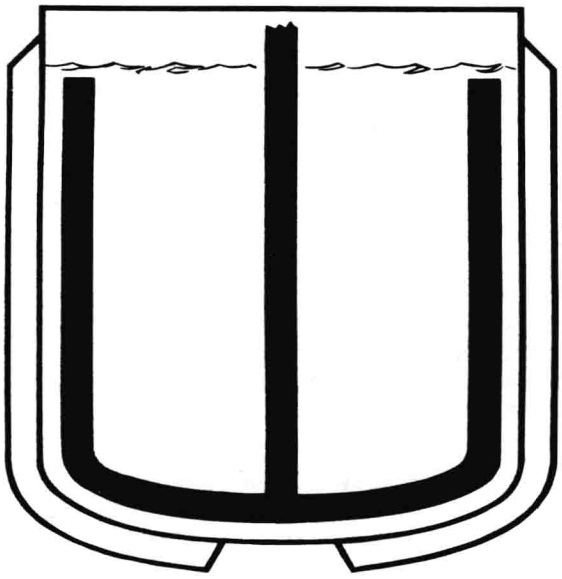

FIGURE 4. Typical anchor impeller.

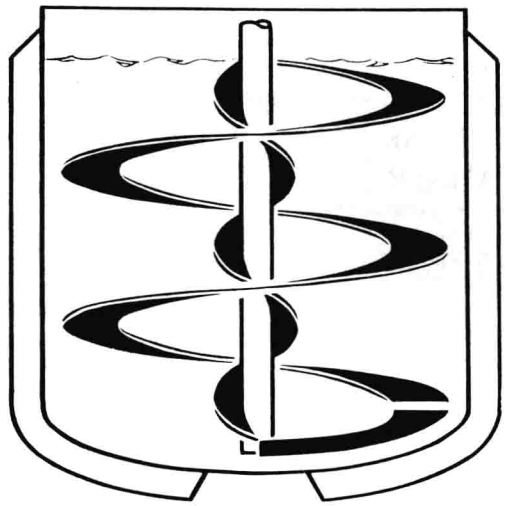

FIGURE 5. Typical helical impeller.

A Variable Volume Two-Zone Mixing Model

S.J. GIBBS
D.F. LOY
K.A. DEBELAK
R.D. TANNER
Department of Chemical Engineering
Vanderbilt University
Nashville, Tennessee 37235

An analysis is presented to determine the dilution rates in a two-zone mixing model when the volumes in each zone are unequal and constant. Also, a model is developed to account for the effect of variable volume mixing zones. The model describes the effect of imperfect mixing on the progress of a first-order irreversible reaction in a batch reactor. The model is described by a system of two nonlinear differential equations. The equations are solved numerically for various values of the mixing parameters in order to study the qualitative effects on the behavior of the model. The variable volume model was qualitatively confirmed by the shape of experimental crossplots of the concentration of reactant in one zone versus the concentration of reactant in the other zone. In addition, the model was tested by comparison with data from an imperfectly mixed batch reactor in which the progress of a pseudo-first-order irreversible reaction was studied.

The two zone mixing model describing the effect of imperfect mixing on a first order irreversible reaction in a batch reactor was developed in two earlier papers (1,2). The model system consisted of a two-zone reactor with equal constant volumes and flow rates, as seen in Figure 1. In another previous paper (3), we studied the effect of constant unequal volumes on the progress of the irreversible A-->B reaction occurring in each zone. In this paper we will present a procedure to determine the dilution rates when the volumes are unequal and constant, and derive a model for the case of a variable volume in the mixing zones. This two zone, variable volume mixing model may have application to both chemical and biomedical models. For example, in many bioprocesses, the effect of poor mixing can be more of a problem at large scale than at small scale because of local buildups, of either product or substrate, leading to product or substrate inhibition. Toxicity caused by excessive concentrations of either products or substrates causes a similar set of problems (4)

In addition, since the model is based on positional differentiation by zones, those bioprocesses which produce thickening agents like gum xanthan or microbial cellulose (biopolymers) can lead to process control problems which arise from the dilemma that some parts of bioreactor are quite fluid while others are viscous (4). When sensors are placed in the bioreactor in different locations they give drastically different information (4). Simple mixing models such as those described in this paper may help deal with such difficulties.

CONSTANT AND UNEQUAL VOLUMES

The equations relating the concentrations in each mixing zone for the irreversible A--> B reaction resulting from the solution of the material balances on zones one and two are (3):

$$A_1 = \frac{A^*}{D_1+D_2}\left[D_1 e^{-(k+D_1+D_2)t} + D_2 e^{-kt}\right] \quad (1)$$

$$A_2 = \frac{A^* D_2}{D_1+D_2}\left[e^{-kt} - e^{-(k+D_1+D_2)}\right] \quad (2)$$

Subtracting Equation (2) from Equation (1) gives the equation relating the concentrations of A in each zone.

$$A_1 = A_2 + A^* e^{(-k+D_1+D_2)t} \quad (3)$$

where,
A_1 = Concentration of A in zone 1 (mol/l)
A_2 = Concentration of A in zone 2 (mol/l)
A^* = Initial Concentration of A in zone 1 (mol/l)
D_i = Interzone flow rate, F, divided by zone volume, V_i, F/V_i, (min^{-1}), the mixing parameter
k = first-order reaction rate constant, (min^{-1})
F = flow rate, (l/min)
V_i = Volume in each zone, i=1,2

For the case where no reaction takes place, k equals zero and

$$A_1 = A^* - \frac{D_1}{D_2} A_2 \qquad (4)$$

This is a line with slope $-D_1/D_2$ and intercept A^*. Equations (3) and (4) can be used to estimate D_1 and D_2 for this ideal case. If the first-order reaction rate constant, k, is known, then the sum $D_1 + D_2$ can be evaluated in this simplified model by taking the natural log of Equation (3) and rearranging

$$\ln\left[\frac{1}{A_1 - A_2}\right] = (k+D_1+D_2)t + \ln\frac{1}{A^*} \qquad (5)$$

From the slope of the $\ln(1/(A_1 - A_2))$ versus time plot, we can find $(k+D_1+D_2)$. The initial concentration of reactant in zone 1 can be found or verified from the intercept. By subtracting the known value of k from $(k+D_1+D_2)$ we can find (D_1+D_2). Obtaining D_1/D_2 for the non-reacting case allows us to calculate the individual dilution rates D_1 and D_2.

Figure 2 shows a crossplot of concentrations for experimental data taken from the crystal violet-sodium hydroxide system. Both the reaction and no reaction cases are shown. The experimental system used to study this pseudo-first order system was previously described (2). From the slope of the no reaction case, the ratio D_1/D_2 is determined to be 1.22, if the initial transient data are neglected ($A_2 < 0.3$). The data for the reaction case are replotted in Figure 3 according to Equation (5) to determine $(k+D_1+D_2)$. The value of k, the pseudo-first order rate constant, at 20°C and a sodium hydroxide concentration of 0.01M was reported to be 3.42×10^{-3} sec^{-1}, from Cosaro (5). The values of D_1 and D_2 are therefore calculated to be 0.247 sec^{-1} and 0.203 sec^{-1}, respectively. The value of A^* can be estimated from either the extrapolated intercept of Equation (4) or from the intercept of Equation (5). The value of A^* determined from Equation (4) was 1.4×10^{-5} gmoles/l and from Equation (5) 1.55×10^{-5} g moles/l. The mismatch of the constant volume model fit for A_2 0.3 and A^* prediction are due to the inadequacy of the constant volume model. These facts support the argument for the development of a more comprehensive model, hence the use of variable volumes in the following section.

THE VARIABLE VOLUME MODEL

In this model, an imperfectly mixed batch reactor is thought of as two perfectly mixed batch reactors which exchange fluid at rates F_1 and F_2 as shown in Figure 1. The basic assumptions in the development of the model are that the flow rates F_1 and F_2 can be described by:

$$F_1 = D_1 V_1 \qquad (6)$$
$$F_2 = D_2 V_2, \text{ where } D_1 \text{ and } D_2 \text{ are constants} \qquad (7)$$

and that the reaction is first-order and irreversible. A material balance on zones 1 and 2 yields the equations under isothermal conditions:

$$\frac{dV_1}{dt} = F_2 - F_1 = D_2V_2 - D_1V_1 \quad (V_1)_0=V_{10} \qquad (8)$$

$$\frac{dV_2}{dt} = F_1 - F_2 = D_1V_1 - D_2V_2 \quad (V_2)_0=V_{20} \qquad (9)$$

where:
V_1 = the volume of zone 1 at anytime
V_2 = the volume of zone 2 at anytime
then, V_1 and V_2 can be found as functions of time, given the initial conditions: V_{10} and V_{20}.

$$V_1 = \frac{D_2V_T}{D_1+D_2}\left[1-e^{-(D_1+D_2)t}\right]+V_{10}e^{-(D_1+D_2)t} \qquad (10)$$

$$V_2 = \frac{D_1V_T}{D_1+D_2}\left[1-e^{-(D_1+D_2)t}\right]+V_{20}e^{-(D_1+D_2)t} \qquad (11)$$

where $V_T = V_1 + V_2$

A balance on component A in Zone 1 yields the equation:

$$\frac{d(V_1A_1)}{dt} = -kA_1V_1 - F_1A_1 + F_2A_2 \quad (12)$$

Expanding $d(V_1A_1)/dt$ and combining the resulting expression with Equations (6)-(8) gives another relationship for $d(A_1V_1)/dt$

$$\frac{d(V_1A_1)}{dt} = (F_2 - F_1)A_1 + \frac{dA_1}{dt} V_1 \quad (13)$$

Setting Equations (12) and (13) equal gives an expression in which V_1 is not differentiated.

$$(F_2-F_1)A_1 + \frac{dA_1}{dt} V_1 = -kA_1V_1 - F_1A_1 + F_2A_2 \quad (14)$$

Using Equations (6) and (7) and the fact that $V_1 + V_2 = V_T$, Equation (14) can be simplified to:

$$\frac{dA_1}{dt} = -kA_1 + (A_2 - A_1) \left[\frac{D_2V_T}{V_1} - D_2\right] \quad (15)$$

Analogously, in zone 2, the differential equation for A_2 becomes:

$$\frac{dA_2}{dt} = -kA_2 + (A_1 - A_2) \left[\frac{D_1V_T}{V_2} - D_1\right] \quad (16)$$

Equations (10),(11),(15), and (16) describe the variable volume two zone mixing model.

The Early Time Approximation

It is difficult to find an analytical solution to Equations (10),(11),(15) and (16) because V_1 and V_2 are such complex functions. However, if Equations (10) and (11) are linearized in time and other approximations are made, one can derive an analytical solution.

First, linearize V_1 and V_2 about t=0.

$$V_1 = V_{10} + \left.\frac{dV_1}{dt}\right|_{t=0} \cdot t \quad (17)$$

$$V_2 = V_{20} + \left.\frac{dV_2}{dt}\right|_{t=0} \cdot t \quad (18)$$

$$\left.\frac{dV_1}{dt}\right|_{t=0} = D_2V_T - V_{10}(D_1+D_2) \quad D_2V_T \quad (19)$$

$$\left.\frac{dV_2}{dt}\right|_{t=0} = D_1V_T - V_{20}(D_1+D_2) \quad -D_2V_T \quad (20)$$

The approximations in Equations (19) and (20) can be viewed as setting $(D_1)_0=(D_2)_0$ and $V_{10} << V_{20}$ in Equations (8) and (9). Therefore,

$$V_1 = V_{10} + [D_2V_T - V_{10}(D_1+D_2)]t \quad (21)$$
$$= V_{10} + [V_{20}D_2 - V_{10}D_1]t$$

and

$$V_2 = V_{20} + [D_1V_T - V_{20}(D_1+D_2)]t \quad (22)$$
$$= V_{20} + [V_{10}D_1 - V_{20}D_2]t$$

Substitution of Equations (21) and (22) into Equations (15) and (16) yields

$$\frac{dA_1}{dt} = -kA_1 \quad (23)$$
$$+(A_1-A_2) \left[\frac{D_2V_T}{V_{10} + [V_{20}D_2 - V_{10}D_1]t} - D_2\right]$$

and

$$\frac{dA_2}{dt} = -kA_2 \quad (24)$$
$$+(A_1-A_2)\left[\frac{D_1V_T}{V_{20} + [V_{10}D_1 - V_{20}D_2]t} - D_1\right]$$

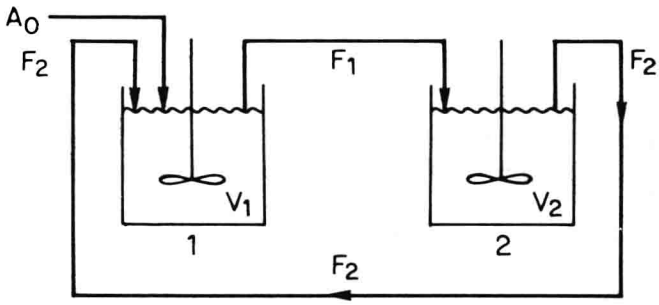

FIGURE 1. Idealized model of a two-zone batch reactor.

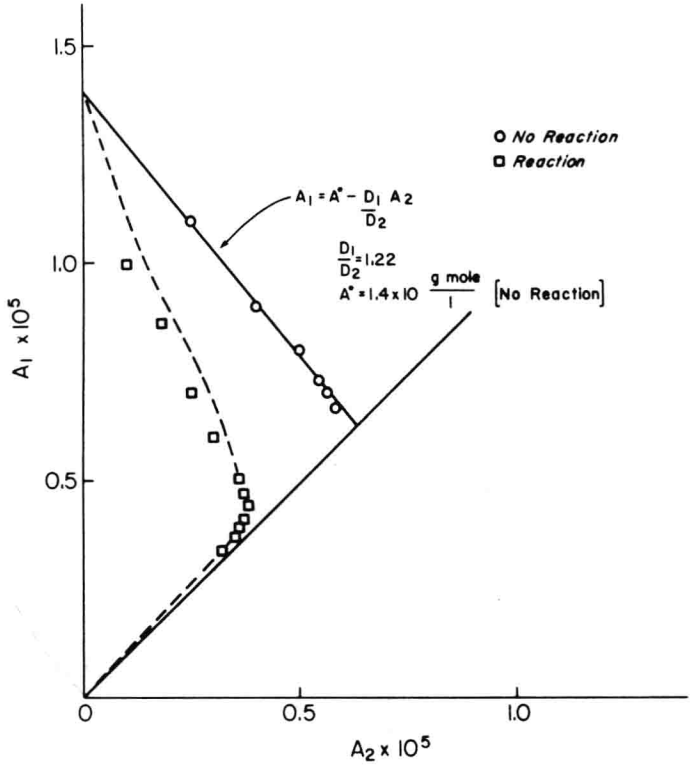

FIGURE 2. Crossplot of concentration of crystal violet dye in zone 1 versus concentration of crystal violet dye in zone 2 for the reaction and no reaction cases.

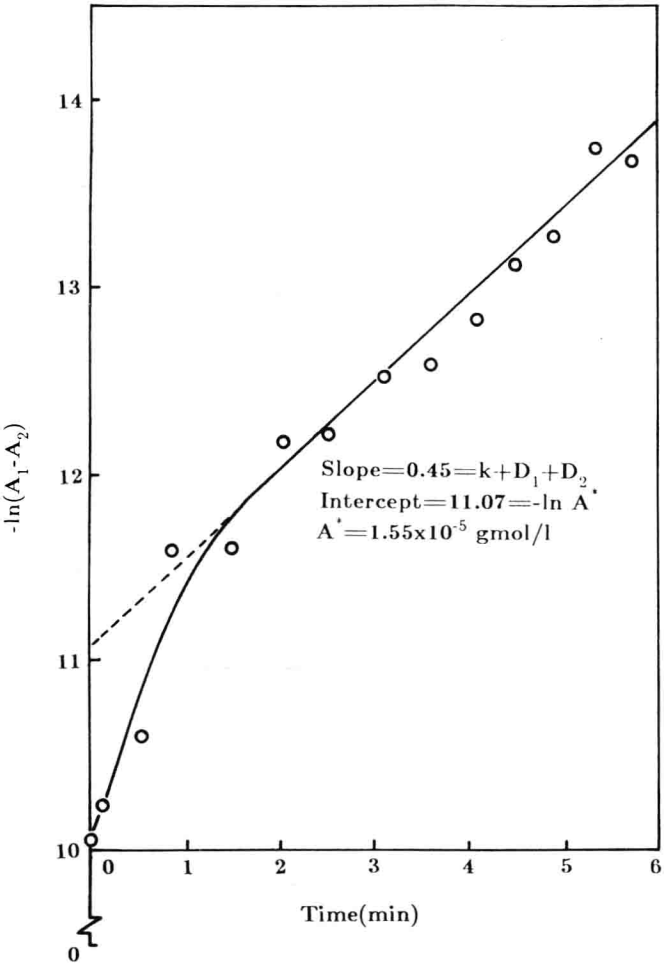

FIGURE 3. Reaction data replotted according to equation (5) to determine ($k + D_1 + D_2$) which equals the slope in the constant volume model.

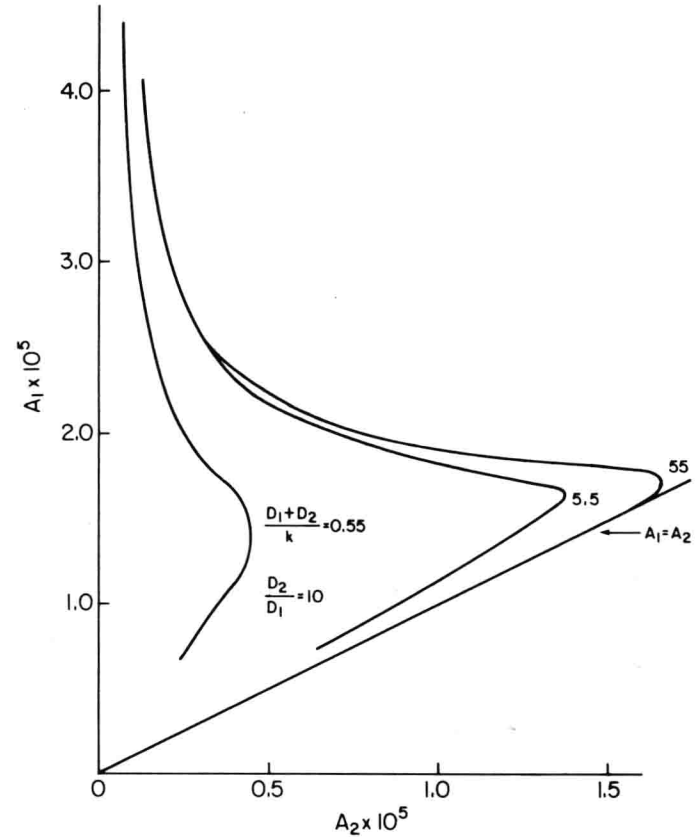

FIGURE 4. Effect of changes in $(D_1 + D_2)/k$ on the crossplot of concentration of A in zone 1 versus concentration of A in zone 2. Simulated variable volume model.

Then, application of Picard's iteration, where

$$A_{10} = A^* \text{ and } A_{20} = 0 \quad \text{gives}$$

$$A_1 = A^* - kA^*t + A^*D_2t - \frac{A_1D_2V_T}{[V_{20}D_2 - V_{10}D_1]} \cdot \ln \frac{V_{10} + [V_{20}D_2 - V_{10}D_1]t}{V_{10}} \quad (25)$$

$$A_2 = -A^*D_1t + \frac{A^*D_1V_T}{[V_{10}D_1 - V_{20}D_2]} \cdot \ln \frac{V_{20} + [V_{10}D_1 - V_{20}D_1]t}{V_{20}} \quad (26)$$

Since the argument of the ln function approaches 1 as time goes to zero, the ln[x] can be approximated by x-1. Therefore, Equations (25) and (26) can be approximated by

$$A_1 = A^* - kA^*t + A^*D_2t - \frac{A_1D_2V_T}{V_{10}}t \quad (27)$$

and

$$A_2 = -A^*D_1t + \frac{A^*D_1V_T}{V_{20}}t \quad (28)$$

Simplification of Equations (27) and (28) yields

$$A_1 = A^* - [k + \frac{V_{20}D_2}{V_{10}}]A^*t \quad (29)$$

$$A_2 = A^*D_1 \frac{V_{10}}{V_{20}} t \quad (30)$$

Thus, if early time data of A_1 and A_2 are available, then the parameters D_1 and D_2 can be estimated from the initial slopes of A_1 and A_2 versus time curves. However, it is generally difficult to obtain enough data at early times to clearly determine values of the initial slopes. Subtracting Equation (30) from Equation (29) gives the analogous relationship to Equation (5) for the variable volume case at early times:

$$\ln\left(\frac{1}{A_1 - A_2}\right) = [k + \frac{V_{20}D_2}{V_{10}} + \frac{V_{10}D_1}{V_{20}}]t + \ln\frac{1}{A^*} \quad (31)$$

Qualitative Features of Crossplots of A_1 vs. A_2

Values for A_1 and A_2 were determined by numerically solving Equations (10),(11),(15), and (16), using the IMSL subroutine DVERK. The numerically simulated equations were used to generate values which could be qualitatively compared to experimental data and used to determine the effect of changing the parameters D_1 and D_2 on the shape of the A_1 vs A_2 crossplot. Typical distinguishing shapes of the A_1 vs A_2 crossplot for the variable volume model are shown in Figures 4 and 5.

Several combinations of values of D_1, D_2, V_{10}, and k were tried in the simulation program and used to develop these crossplots of A_1 vs. A_2. In comparing these curves with the constant volume case in Figure 2, it is evident that the variable volume model simulations lead to a more distinct peak (representing a rapid rise in concentration in the second zone) than does the constant volume model.

Parameter Estimation

If plots of A_1 and A_2 versus time are made for experimental data, the values of A_1, A_2, dA_1/dt and dA_2/dt can be determined for various values of time. The values of the groups $[(D_2V_T/V_1) - D_2]$ and $[(D_1V_T/V_2) - D_1]$ can be determined at various time values. The values of D_1 and D_2 can also be estimated using a computer assisted trial and error solution of Equations (10) and (11) given the values of the above two groups at a specific time.

The experimental set-up used to obtained data to test the variable volume model differed from previous work in that a single stirrer was used as opposed to two stirrers. Two mixing speeds: 106 rpm and 75 rpm were studied, and the reaction vessel volume was larger: 8 liters as opposed to 1 liter. Otherwise, the procedure was similar to that previously used (2). Plots of experimental data and simulations based on values of D_1 and D_2, determined from the trial and error method, are shown in Figures 6 to 8. The simulation corresponds well with one set of